On the relations between ISE and structure in some RE(Mg)SiAlO(N) glasses

Keding, Ralf; Dauce, Rachel; Sangleboeuf, J. C.

Published in:
Journal of Materials Science

DOI (link to publication from Publisher):
10.1007/s10853-008-2851-3

Publication date:
2008

Document Version
Publisher's PDF, also known as Version of record

J Mater Sci (2008) 43:7239–7246
DOI 10.1007/s10853-008-2851-3

On the relations between ISE and structure in some RE(Mg)SiAlO(N) glasses

R. Daucé · R. Keding · J.-C. Sangleboeuf

Received: 31 July 2007 / Accepted: 1 July 2008 / Published online: 23 September 2008

Abstract Six oxide and oxynitride glasses were synthesized in the Y–Mg–Si–Al–O–N, Nd–Mg–Si–Al–O–N and La–Mg–Si–Al–O–N systems. As already known, nitrogen introduction increases the T_g, packing factor and mechanical properties of the glasses. Cationic substitution also has an influence on the glasses' behavior, particularly in terms of sensitivity to indentation load/size effect (ISE). The structure of the yttrium-containing glasses was investigated by mean of ^{27}Al and ^{29}Si MAS-NMR. Al is found to occur for 2/3 as a network former and for 1/3 as a modifier. The oxide glass mainly contains Q^2 and Q^3 silicate units and SiO_3N and SiO_2N_2 units are created when nitrogen is introduced into the glass network. The average number of rigid bonds per network former $\langle n \rangle$ was calculated from the glasses' composition. A discrepancy between $\langle n \rangle$ and the Raman spectra of the glasses suggests that parts of the magnesium behaves as a former in the network. $\langle n \rangle$ seems to be a key parameter governing hardness and sensitivity to ISE and can be linked to normal/abnormal behavior of glasses regarding indentation.

Introduction

The sintering of aluminosilicate oxynitride ceramics requires additives like MgO or Y_2O_3 and leads to the formation of glassy phases at the grain boundary. SiAlON glasses were consequently widely studied in order to improve the resistance of SiAlON ceramics, particularly at high temperatures. SiAlON glasses are also of interest in radioactive waste management as their good chemical durability makes them suitable for storage via vitrification of the wastes [1, 2]. Due to their thermal properties associated with their ability to incorporate chemical analogues of actinides in their composition, they are candidates for studying the effects of actinides transmutation on glasses. Before any attempt of irradiation, a good knowledge of their properties and their structure is required.

Literature shows that the introduction of nitrogen into silicate and aluminosilicate glasses increases their T_g, elastic modulus, hardness and melt viscosity [3–11]. In terms of structure, Si and Al are considered to be typical network formers covalently linked via oxygen or nitrogen atoms. In this covalent network, metallic modifiers create non-bridging oxygen atoms (NBO, the occurrence of non-bridging nitrogen has been more seldom reported) [12–24].

Hardness is a test easy to perform. It allows to probe the materials' surface, an important feature in the case of external irradiations which will modify the glass only to a depth of 100 μm. However, several parameters can possibly lead to a decrease of the material hardness when the testing load is increased. This phenomenon, generally referred to as the indentation size/load effect (ISE) [25–30], has been tentatively described by several models:

(i) the elastic recovery model: the length of the trace's diagonal upon loading is obtained by adding a correction term δ to the measured value d. The relation between the load P and d can consequently be expressed as:

$$P = a(d + \delta)^2 \quad (1)$$

where a is a term related to load-independent hardness. However, the range of the applied loads or the

R. Daucé (✉) · J.-C.Sangleboeuf
LARMAUR, FRE CNRS 2717, Université de Rennes 1,
35042 Rennes Cedex, France
e-mail: rachel.dauce@gmail.com

R. Keding
Chemistry and Environmental Engineering, Aalborg University,
Aalborg, Denmark

polishing processes are of much influence on δ [26], leading relation (1) to be non-valid in most cases.

(ii) the energy balance model: initially developed by Bernhardt, this model states that the total indentation work $W = \int P \cdot dh$ can be divided into two parts:

– the work corresponding to the volume deformation:

$$W_1 = \int P_1 \cdot dh = ad^3 \quad (2)$$

– the work corresponding to surface creation:

$$W_2 = \int P_2 \cdot dh = bd^2 \quad (3)$$

where h represents the penetration depth of the indenter, a and b are constants. Differentiating these equations leads to a general microhardness law of the type

$$P = a_1 d + a_2 d^2 \quad (4)$$

where a_1 is a term related to surface creation and a_2 a term related to volume deformation.

(iii) the proportional specimen resistance: the a_1 value being too high to be explained by facets creation only, Li and Bradt [27] used a model mathematically similar but with a different physical meaning. According to them, a_1 would reflect the resistance of the tested specimen, which is directly proportional to the indentation size.

The work of several authors on ceramics or glasses [28, 31–35] showed, however, that fracture occurs to some extent when the indentation load is increased. This crack formation increases the area of surface created during indentation, leading to high a_1 values.

The sensitivity to ISE of the six studied glasses was investigated using a $P/d = f(d)$ curve. The a_1 values obtained are discussed with regards to the indentation topology and the structure of the glass.

Experimental

Glass synthesis and characterization

The compositions of the glasses studied are reported in Table 1. SiO_2, Ln_2O_3, $MgSiO_3$, Al_2O_3 powders (reagent grade) were dried at 800 °C for 12 h. For the oxynitride compositions, part of Al_2O_3 was replaced by AlN. Powders were weighted and mixed for 1 h in a glass bottle. The raw mixtures were molten for 1 h in a molybdenum crucible in an induction furnace under high-purity nitrogen atmosphere. The melt was quenched and then crushed in coarse pieces. Glass powders of a granulometry <20 μm were obtained by milling and sieving. The powders were pressed to pellets by uniaxial hot pressing in a carbon mould. The mould was heated with a heating rate of 10 °C/min to the pressing temperature (T_g + 50 °C). A 10 MPa pressure was applied during 45 min before 1 h annealing at the glass transition temperature followed by a slow decrease to room temperature (2 °C/min). This shaping stage allowed to obtain homogeneous and stress-free pellets, which were then cut and mirror polished with a diamond paste.

Table 1 Compositions of the studied glasses (mol%)

Glass	Nd_2O_3	La_2O_3	Y_2O_3	MgO	SiO_2	Al_2O_3	Si_3N_4
YMG			7.88	20.34	52.64	19.14	
YMGN			8.72	22.50	42.30	21.17	5.31
NDMG	11.53			20.00	50.51	17.97	
NDMGN	12.62			22.22	40.54	19.68	4.95
LAY		10.00	10.00		60.00	20.00	
LAYN		11.12	11.12		49.94	22.25	5.56

All the glasses are amorphous according to the X-ray diffraction (XRD) pattern and no crystalline impurities were evidenced using scanning electron microscopy (SEM).

The cationic contents were determined by chemical analysis (ICP-EOS) after digestion in soda-potash. The nitrogen and oxygen contents were measured by combustion analysis (LECO). The measured compositions are in good agreement with the ones of the raw mixes.

The specific mass ρ of the crushed glasses was determined using a helium pycnometer (Micromeritics). Ten recordings were performed for each sample. The packing factor C for each composition was calculated according to the following equation:

$$C = \frac{\sum x_i \cdot V_i}{(\sum x_i \cdot m_i)/\rho} \quad (5)$$

where x_i, V_i and m_i are respectively the atomic fraction, the volume [36] and the atomic mass of the ith element.

The glass transition temperatures were obtained by differential thermal analysis (SETARAM) on the glass powders, in a platinum crucible, under flowing nitrogen, with a heating rate of 10 °C/min.

The elastic moduli were calculated from the longitudinal and transverse ultrasonic wave velocities (respectively V_L and V_T), measured with 10 MHz-piezoelectric transducers.

Hardness testing was performed with loads ranging from 0.25 to 19.62 N (ten indentations for each load). Meyer's hardness and a_1 were obtained from the $P/d = f(d)$ plots.

Raman spectroscopy

Raman spectra were recorded using a TiSa laser (812 nm) in order to avoid a continuous background caused by glass

fluorescence for incident radiations of 488 nm and 514 nm (Argon laser) and 720 nm (TiSa laser). The laser line was filtered by a monochromator, and the power on the sample was limited to 3 mW. All the spectra were recorded, with a Dilor XY spectrometer and normalized on the Raman band around 950 cm^{-1}.

Nuclear magnetic resonance spectroscopy

^{29}Si and ^{27}Al MAS-NMR spectra of yttrium-containing glasses YMG and YMGN were recorded with an ASX300 (7T) Bruker spectrometer. Resonance frequencies for Si and Al are of 59.6 and 78 MHz, respectively. For the ^{27}Al NMR spectra the spinning rate at magic angle was 15 kHz with an excitation pulse of 1 μs and a delay of 1 s between two acquisitions. For the ^{29}Si NMR spectra, the spinning rate was 8 kHz, with an excitation pulse of 2 μs and a delay time of 30 s. A total of 1024 spectra were accumulated for Al and 7500 for Si. References for chemical shifts were aqueous solution of 1 M of $Al(NO_3)_3$ for Al, and TMS for Si. Error on chemical shift values is estimated to ±1 ppm. All spectra were analyzed using the DM2002 software [25].

Results

Properties

Properties of the glasses are gathered in Table 2. The most important parameter influencing the glasses' properties is, as expected, the presence of nitrogen. Glasses are harder, more rigid, more compact and exhibit higher glass transition temperatures. Cationic substitution is of influence on the properties too. The LAY(N) glasses exhibit the highest Young's modulus but comparatively low hardness, while the YMG(N) glasses have the lowest Poisson's ratio. One noticeable fact is the evolution of the a_1 parameter, related to size/load effect susceptibility. Whereas YMGN and NDMGN show no ISE ($a_1 \approx 0$), LAY, LAYN and NDMG roughly exhibit the same a_1 value. YMG has an intermediate a_1 value.

Table 2 Properties of the studied glasses

Glass	YMG	YMGN	NDMG	NDMGN	LAY	LAYN
T_g (°C) ± 5	835	845	820	850	875	918
ρ (g cm^{-3}) ± 0.001	3.052	3.183	3.740	3.804	3.741	3.843
Packing factor	0.405	0.426	0.432	0.442	0.424	0.437
E (GPa) ± 2	107	124	109	119	114	124
G (GPa) ± 1	44	49	42	46	45	48
K (GPa) ± 3	66	86	83	99	86	98
v	0.23	0.26	0.28	0.30	0.28	0.29
H_{Meyer} (GPa) ± 0.1	7.9	9.5	7.3	8.9	7.1	8.6
a_1 (N/mm)	6.4	1.6	10.2	−0.6	9.6	9.6
$\langle n \rangle$	2.71	2.96	2.37	2.61	2.46	2.69

Structure

Anionic substitution effect on the silicon environment

In both the oxide YMG and the oxynitride glasses, the shoulder located around 740 cm^{-1} on the Raman spectrum (Fig. 1) can be attributed either to the Si–O–Si or to the Si–O–Al bonds vibrations [37]. The two intense bands at 925 and 1025 cm^{-1} are assigned to the Si–O stretching vibrations in SiO_4 tetrahedra with respectively two and one NBO (Q^2 and Q^3 units) [20, 38]. No band is evidenced in the domain of Si–O stretching modes in Q^1 or Q^0 units. The Q^3/Q^2 ratio in YMGN is clearly smaller than in YMG. The 1115 cm^{-1} shoulder is attributed to Si–O stretching in fully connected tetrahedra in YMG (Q^1), probably overlapped with Si–N vibrations in the case of YMGN [20]. The two shoulders at 1250 and 1450 cm^{-1} are supposed to be due to point defects.

^{29}Si NMR provides more accurate data on the silicon environment in glasses. The spectra for both YMG and YMGN, represented on Fig. 2, were simulated using Gaussian–Lorentzian components in order to evaluate the contributions of the different silicate units.

In YMG, the main contributions in the signal are located around −83 and −91 ppm and attributed to Q^2 and Q^3 units, respectively [23]. Considering Raman spectra, a contribution of the Q^4 units was added in the YMG spectrum simulation. Regarding the simulation results (Table 3), Q^4 units represent about 6% of the silicate tetrahedra. According

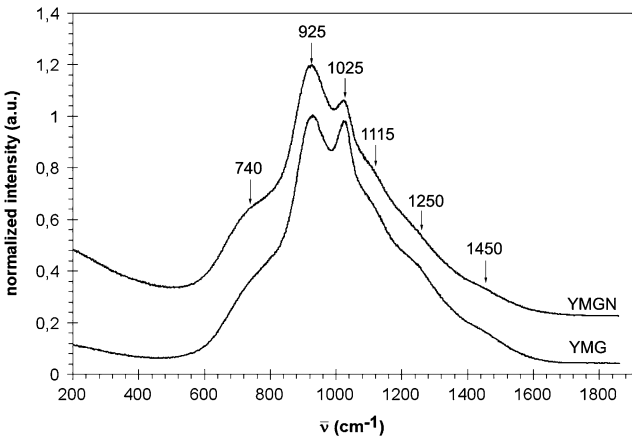

Fig. 1 Raman spectra of the oxide glass YMG and its oxynitride equivalent YMGN

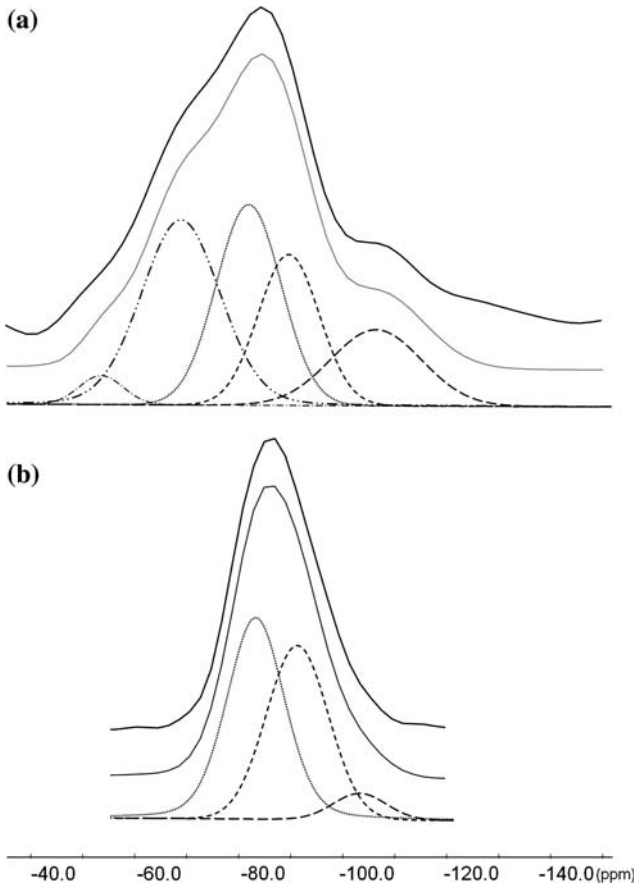

Fig. 2 ^{29}Si NMR spectra of (**a**) the oxide glass YMG and (**b**) its oxynitride equivalent YMGN. Dotted lines indicate the simulated contributions

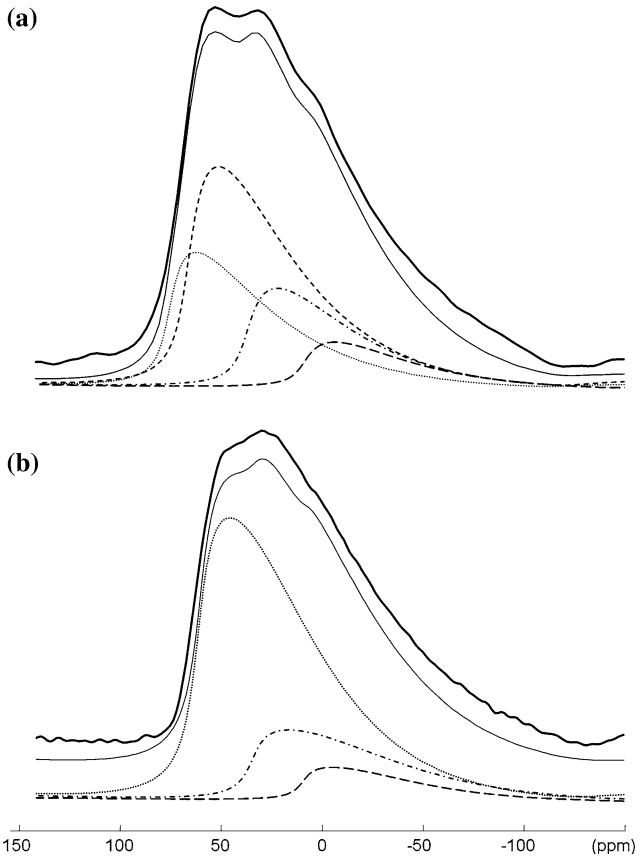

Fig. 3 ^{27}Al NMR spectra of (**a**) the oxide glass YMG and (**b**) its oxynitride equivalent YMGN. Dotted lines indicate the simulated contributions

Table 3 ^{29}Si NMR spectra simulation results for both YMG and YMGN

Glass	Structural unit	δ (^{29}Si) (ppm) ± 0.1	FWHM (ppm) ± 0.1	Population (%) ± 1
YMG	Q^2	−83.1	12.9	50
	Q^3	−91.0	14.1	44
	Q^4	−102.9	12.1	6
YMGN	SiO_2N_2	−55.7	7.8	4
	SiO_3N	−69.3	17.0	37
	Q^2	−82.5	12.9	28
	Q^3	−91.1	14.9	21
	Q^4_{0Al}	−107.9	18.5	9

to the chemical shift, one or two aluminium atoms are present in their second coordination sphere [23]. Q^2 and Q^3 units are present in comparable amounts in YMG ($Q^3/Q^2 \approx 0.9$).

The presence of nitrogen in the glass causes an increase of the relaxation time of the silicon [23], leading to long acquisition times and a comparatively lower signal/noise ratio than in the case of pure oxide glasses. As a consequence realistic simulations are more difficult to perform. Contributions of Q^4, $[SiO_3N]$ and $[SiO_2N_2]$ units, which are located at the very ends of the spectrum, are particularly sensitive toward errors in interpretation. Still, introduction of nitrogen in YMGN brings a wider variety in silicon environment: two new bands appear around −70 and −58 ppm, which are attributed to $[SiO_3N]$ and $[SiO_2N_2]$ units [12]. Chemical shifts, FWHMs and percentages of each structural unit are summarized in Table 3. Mainly SiO_3N tetrahedra are created by introducing nitrogen in the glass (nearly 40% of the total population) but probably also a small amount of SiO_2N_2. Q^4 tetrahedra seem to be present in the same amount than in the oxide glass, but their chemical shift is moved toward lower ppm values. The number of both Q^3 and Q^2 is decreased in comparison to YMG and the Q^3/Q^2 ratio is changed approximately to the value of 0.75.

The central transition of ^{27}Al-MAS spectra for YMG and YMGN is shown in Fig. 3. These two spectra exhibit several components associated with the typical asymmetrical line shapes observed in glasses when second order quadrupolar effects occur. The calculation model assumes a Gaussian distribution of the quadrupolar constant ν_Q for all the components of each spectrum. Three contributions

Table 4 ^{27}Al NMR spectra simulation for YMG and YMGN

Glass	Structural unit	δ (^{27}Al) (ppm) ± 0.1	Population (%) ± 2
YMG	Al_{IV}	60.5	71
	Al_{V}	33.5	21
	Al_{VI}	8.5	8
YMGN	AlO_3N	77.0	27
	AlO_4	68.5	44
	Al_{V}	38.9	20
	Al_{VI}	10.1	9

were found for YMG (around 60, 33, and 8 ppm) which were attributed to aluminium in four-, five- and six-fold coordination, respectively [13]. According to simulation results (Table 4), one-third of the aluminum atoms are present as glass modifiers in YMG, in six- or five-fold coordination. The two other thirds are tetrahedrally coordinated and are part of the formative network.

The YMGN glass spectrum is slightly different: a weak contribution with an isotropic chemical shift around 110 ppm appears and can be attributed to AlN_4 tetrahedra [17, 39]. Moreover, a dissimilarity exists between YMG and YMGN signals for high ppm values. A contribution with an isotropic chemical shift around 77 ppm was added in the simulation to take it in account, which allows to obtain a better agreement between the calculated and the experimental spectra. This contribution is likely to be caused by the [AlO_3N] tetrahedra [39].

Cationic substitution

The Raman spectra of the three oxynitride glasses, recorded between 840 and 1150 cm^{-1}, are shown in Fig. 4. A vibration located around 1025 cm^{-1} is present for all glasses and is supposed to be related to the Q^3 units. The

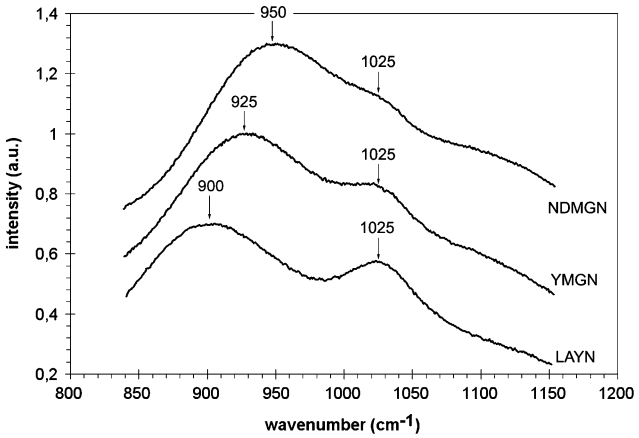

Fig. 4 Influence of the cationic substitution on the oxynitride glasses Raman spectra. The three glasses clearly exhibit different degrees of polymerization

vibration around 925 cm^{-1} associated to Q^2 units in YMGN is shifted by 25 cm^{-1} toward lower wavenumbers in the case of NDMGN. The broadness of the band indicates that a contribution of Si–O stretching from the Q^1 units could exist. This phenomenon is just more obvious in LAYN spectrum which shows a very broad band centered at 900 cm^{-1} probably caused by two different contributions (Si–O stretching from Q^2 and Q^1 units).

Discussion

The role of nitrogen is comparatively easy to evaluate. As reported previously [3, 5, 7, 40–42], nitrogen increases the average polymerization of the network which leads to an increase of T_g, of the packing factor and of the mechanical properties. The effect of the cationic substitution is, however, more difficult to grasp. On one hand, the LAY(N) glasses exhibit the highest elastic properties but they also have the lowest hardness values and both LAY and LAYN are sensitive to ISE. On the other hand, the YMG(N) glasses exhibit low bulk modulus and for both the YMG(N) and the NDMG(N) systems the oxynitride glass is insensitive to load/size effects whereas the oxide equivalents exhibit ISE.

According to the results of the structural analysis, aluminium is found for 2/3 as a network former (CN = 4) and for 1/3 as a network modifier (CN = 5, 6) in the YMG(N) system. The distribution in the LAY(N) glasses was reported to be roughly the same [2]. From these proportions, and supposing the distribution of Al is identical in the NDMG(N) system, the average polymerization for the $Si(O,N)_4$ units can be calculated from the composition of the glass, using a generalized Thorpe's constraint model [43–45] as developed by Avramov et al. [46].

According to Thorpe, the average coordination number $\langle r \rangle$ of a glass network can be determined as follows:

$$\langle r \rangle = \frac{\sum_{r=2}^{4} r n_r}{\sum_{r=2}^{4} n_r} \quad (6)$$

where n_r represents the number of atoms with a coordination r. This model devised for chalcogenide glasses states that quenching a melt will not result in a glass for $\langle r \rangle = 2.4$. The chalcogenide elements are supposed to be linked together only via covalent bonds, Thorpe's original model is consequently not applicable to classical silicate glasses. Avramov et al. modified it asserting only network formers participate in the network, being linked by rigid oxygen bridges. Modifiers will convert parts of the covalent bonds into ionic bonds which do not belong to the network and impose minimal constraints compared to rigid covalent bonds. Consequently, to calculate the average number of

rigid bonds per network former, the average number of bonds that impose no constraint $\langle m \rangle$ has to be subtracted from the maximum number of rigid bonds $\langle r \rangle$. $\langle m \rangle$ is defined by Eq. 6:

$$\langle m \rangle = \frac{\sum q s_q}{\sum n_i} \tag{7}$$

where s_q is the number of network modifiers with q non-constraining bonds.

The average number of constraining bonds per building unit $\langle n \rangle$ is consequently defined as follows:

$$\langle n \rangle = \langle r \rangle - \langle m \rangle \tag{8}$$

In a classical silicate glass, $\langle r \rangle$ will be considered to be equal to 4. In case of the oxynitride glasses, however, the presence of nitrogen increases the possible number of Si–(O,N)–Si rigid links per Si. In a SiN_2 unit, the number of rigid bridges between two Si per tetrahedron would be 8. Still, because of charge balance the composition is not Si_3N_6 ($3 \times SiN_2$), but Si_3N_4. As a consequence the value of $\langle r \rangle$ is equal to 5.33.

In an oxynitride silicate glass, $\langle r \rangle$ can be calculated as follows:

$$\langle r \rangle = \frac{4 \times [\mathrm{Si}]_{\mathrm{SiO_2}} + 5.333 \times [\mathrm{Si}]_{\mathrm{Si_3N_4}}}{[\mathrm{Si}]} \tag{9}$$

The presence of aluminum with its intermediate role has to be integrated in Eqs. 6 and 8, considering that each $[AlO_4]^-$ will scavenge one charge from a modifier, preventing the formation of one NBO.

In an aluminosilicate oxynitride with a ratio $\frac{[AlO_4]^-}{Al_V + Al_{VI}} = 2$, $\langle n \rangle$ can consequently be calculated as follows:

$$\langle n \rangle = \frac{4 \times [\mathrm{Si}]_{\mathrm{SiO_2}} + 5.333 \times [\mathrm{Si}]_{\mathrm{Si_3N_4}} + 4 \times \frac{2}{3}[\mathrm{Al}]}{[\mathrm{Si}] + \frac{2}{3}[\mathrm{Al}]} - \frac{2 * [\mathrm{AE}] + 3 * [\mathrm{RE}] + \frac{1}{3}[\mathrm{Al}]}{[\mathrm{Si}] + \frac{2}{3}[\mathrm{Al}]} \tag{10}$$

[AE] and [RE] represent the amount of alkaline-earth and rare-earth modifiers, respectively.

The calculated values of $\langle n \rangle$ are reported in Table 2.

One important point before trying to correlate the structural information with the microhardness data is to identify the deformation mechanism occurring during the indentation process. Classically, silica-rich glasses (with high $\langle n \rangle$ values) exhibit a so-called 'anomalous' behavior governed by a deformation process which occurs mainly by densification of the silicate tetrahedral network. In those glasses, indentation leads to a more close-packed structure. On the contrary, glasses containing a certain amount of modifiers are considered as 'normal' glasses. The modifiers restrict the motion of the bridging bonds and the deformation occurs by a shear flow process. This 'normal' behavior produces a specific indentation trace with 'slip lines' [35, 47]. AFM pictures were recorded for all the glasses, and the example of NDMGN is given in Fig. 5. Shear deformation bands are clearly visible on the faces of the indentation (Fig. 5b), giving the evidence that the glasses behave "normally", i.e. that the deformation takes place by shear flow mechanism. If those shear lines and zones of weaker bonding (non-bridging links between oxygen and modifiers) can be linked, the parameter $\langle n \rangle$, being an estimator of the amount of ionic bonds, would be expected to correlate with the hardness (i.e., $H_{YMG(N)} > H_{NDMG(N)} \approx H_{LAY(N)}$). Whereas this correlation works fine for the oxide glasses, this is not the case for the oxynitride glasses where H_{LAYN} is slightly inferior to H_{NDMGN}. In the same way, the a_1 parameter, characteristic of ISE, should be linked to $\langle n \rangle$. Still, some discrepancies appear:

(i) LAYN, despite having a high $\langle n \rangle$ value, does clearly exhibit ISE.
(ii) $\langle n_{NDMGN} \rangle$ is inferior to $\langle n_{YMG} \rangle$ but NDMGN is insensitive to ISE when YMG is not.

The apparent failure in correlating the calculated $\langle n \rangle$ value and the indentation results can be at least partly explained when considering the role of magnesium. Actually, magnesium has been encountered in various

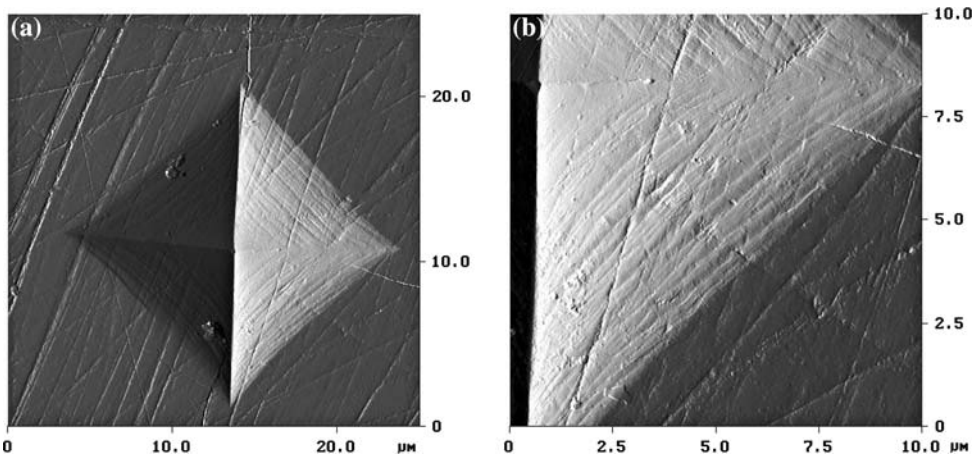

Fig. 5 (**a**) AFM picture of an indentation in NDMGN (10 s/0.981 N) and (**b**) zoom on one of the indentation facets

coordination environments in aluminosilicate glasses (CN = 4–6) and the presence of nitrogen promotes a four-fold coordination for Mg [22]. Thus, Mg is likely to participate in the tetrahedral silicate network. The Raman and NMR spectra come to consolidate this opinion, as visibly the LAYN glass contains more Q^2 and Q^1 units than the YMGN or the NDMGN ones, though they contain the same proportion of Al in a former position [2]. The difference in the amount of non-bridging links consequently does not come from a different $Al_{former}/Al_{modifier}$ ratio. Magnesium being the only other element which can be encountered in four-fold coordination in glasses, the $\langle n \rangle$ parameter is probably underestimated for the Mg-containing glasses, particularly in the case of the oxynitride glasses.

Taking into account this underestimation of $\langle n \rangle$, a correlation appears between it and the a_1 parameter, suggesting a relation between ISE and normal/abnormal behavior of glasses. To check this hypothesis, the glasses were polished into wafers and indented at a load of 19.62 N for 10 s. The wafers were then broken in two parts along the indentation line and the cross section was investigated by means of optical microscopy. It appears clearly that whereas glasses exhibiting ISE develop a net of cracks beneath the indentation (Fig. 6a), those insensitive to ISE (Fig. 6b) behave as an "abnormal" silica-rich glass cracking-wise, showing no cracks. Two important points arise from this observation:

(i) the energy balance model by Bernhardt seems adapted to those glasses. Glasses which do not exhibit cracking below the indentation trace have a_1 parameters close to 0, whereas those sensitive to ISE show a net of cracks beneath the indent. a_1 seems indeed a term related to surface formation.

(ii) there is no well-defined transition between normal and anomalous behavior in those glasses. All glasses exhibit shear lines characteristic of shear-flow deformation in the indentation trace, but cracking-wise, some behave as normal glasses, showing a net of cracks below the indentation, while the most polymerized ones do not.

The Poisson's ratio and bulk modulus values can be likewise understood in terms of polymerization, as highly polymerized glasses with comparatively low packing-factors will be more sensitive to compression. As a consequence, YMG(N) glasses exhibit low K and v values. However, $\langle n \rangle$ alone does not allow to explain the quite similar K and v values for the NDMG(N) and LAY(N) glasses nor the variations in the Young's moduli. More cationic substitution should be done to understand what are the structural key parameters influencing the elasticity of glasses.

Conclusion

The main parameter influencing the glasses' properties is the presence of nitrogen. Additionally, cationic substitution affects the glass behavior by creating NBO in the covalent network. Consequently, the average number of rigid bonds per building unit $\langle n \rangle$ which is estimated from the glass formula can be correlated to the glass properties.

The calculation of $\langle n \rangle$ requires information on the structural building units, as aluminum is an intermediate cation. According to the NMR data, Al is by one third located in a modifying position and by two third in the covalent network as $[AlO_4]^-$ tetrahedra. A discrepancy between the calculated $\langle n \rangle$ values and the Raman spectra of the oxynitride glasses leads to consider that the magnesium exhibit an intermediate behavior too.

Glasses with a high $\langle n \rangle$ show a tendency toward abnormal behavior regarding indentation, showing no cracks beneath the indent. Those glasses are insensitive to ISE. On the contrary, glasses with a lower $\langle n \rangle$ value exhibit a net of cracks under the indentation and their hardness decreases with increase in the applied load. This observation confirms the early theory of Bernhardt that the a_1 parameter in the

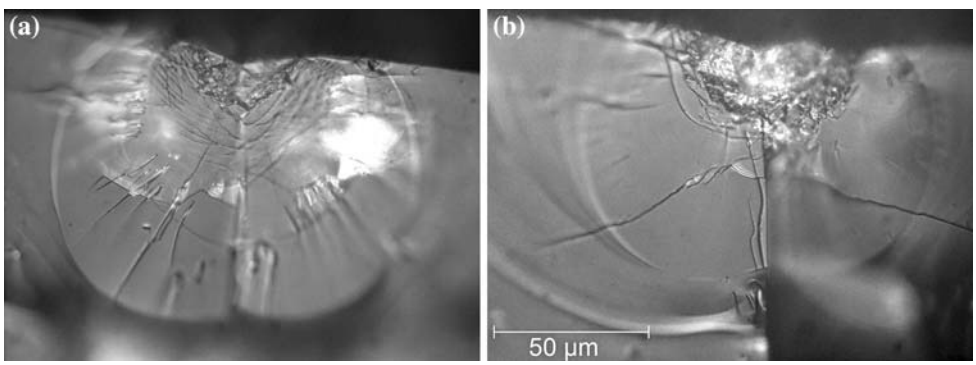

Fig. 6 (**a**) Cross section of an indentation (10 s/19.62 N) in LAYN and (**b**) in NDMGN. LAYN is prone to ISE and exhibit a net of cracks beneath the indentation whereas NDMGN does not

$P = a_1 d + a_2 d^2$ expression is correlated with the surfaces created by indentation.

Acknowledgements Part of this work was financed by a grant from the French atomic energy commission. The authors thank A. Moréac for the Raman spectra acquisition and M. Le Floch for the NMR spectra acquisition and help for the simulation, U. Schmidt and A. Völzke, Max Planck Institute CPFS, Dresden, Germany, for the ICP-OES analysis.

References

1. Leturcq G, Berger G, Advocat T, Vernaz E (1999) Chem Geol 160:39. doi:10.1016/S0009-2541(99)00055-8
2. Guillopé S (1999) Thèse de l'Université de Rennes 1
3. Loehman RE (1979) J Am Ceram Soc 62(9–10):491. doi:10.1111/j.1151-2916.1979.tb19113.x
4. Sakka S, Kamiya K, Yoko T (1983) J Non-Cryst Solids 56:147
5. Ramesh R, Nestor E, Pomeroy MJ, Hampshire S (1997) J Eur Ceram Soc 17:1933. doi:10.1016/S0955-2219(97)00057-5
6. Rocherullé J, Ecolivet C, Poulain M, Verdier P, Laurent Y (1989) J Non-Cryst Solids 108:187
7. Hampshire S, Drew RAL, Jack KH (1984) J Am Ceram Soc 67:C46
8. Makishima A, Mitomo M, Li N, Tsutsumi M (1983) J Am Ceram Soc C55
9. Pastuszak R, Verdier P (1983) J Non-Cryst Solids 56:141
10. Hyatt MJ, Day DE (1987) J Am Ceram Soc 70(10):C283. doi:10.1111/j.1151-2916.1987.tb04901.x
11. Sakka S (1995) J Non-Cryst Solids 181:215
12. Aujla RS, Leng-Ward G, Lewis MH, Seymour EFW, Styles GA (1986) Philos Magn B 54(2):51. doi:10.1080/13642818608239002
13. Engelhardt G, Michel D (1987) High resolution solid-state NMR of silicates and zeolithes. Wiley, New York, pp 143–149
14. Jin J, Yoko T, Miyaji F, Sakka S, Fukunaga T, Misawa M (1994) Philos Magn 70:191. doi:10.1080/01418639408241800
15. Kroeker S, Stebbins JF (2000) Am Miner 85:1459
16. Utegulov ZN, Eastman MA, Prakabar S, Mueller KT, Hamad AY, Wicksted JP, Dixon GS (2003) J Non-Cryst Solids 315:43
17. Mackenzie KJD, Meinhold RH (1994) J Mater Sci 4(10):1595
18. Kohli JT, Condrate RA, Shelby JE (1993) Phys Chem Glasses 34(3):81
19. Kohli JT, Shelby JE, Frye JS (1992) Phys Chem Glasses 33(3):73
20. McMillan P, Piriou B (1983) Bull Mineral 106:57
21. Schneider M, Gasparov VA, Richter W, Deckwerth M, Rüssel C (1997) J Non-Cryst Solids 215:201
22. Videau JJ, Etourneau J, Garnier C, Verdier P, Laurent Y (1992) Mater Sci Eng 15:249. doi:10.1016/0921-5107(92)90066-I
23. Mackenzie KJD, Smith ME (2002) Multinuclear solid-state NMR of inorganic materials. Pergamon
24. Unuma H, Maekawa H, Kiyono H, Kawamura K, Maekawa T, Yokokawa T (1992) J Ceram Soc Jpn 100(11):1292
25. Frohlich F, Grau P, Grellmann W (1977) Phys Status Solidi 42(1):79. doi:10.1002/pssa.2210420106
26. Bückle H (1960) Publications scientifiques et techniques du ministère de l'air, pp 115–121
27. Li H, Bradt RC (1992) J Non-Cryst Solids 146:197
28. Quinn JB, Quinn GD (1997) J Mater Sci 32:4331. doi:10.1023/A:1018671823059
29. Iost A, Bigot R (1996) J Mater Sci 31:3573. doi:10.1007/BF00360764
30. De Graaf D, Braciszewicz M, Hintzen HT, Sopicka-Litzer M, De With G (2004) J Mater Sci 39:2145. doi:10.1023/B:JMSC.0000017777.05637.a6
31. Marshall DB, Lawn BR, Evans AG (1982) J Am Ceram Soc 65(11):561. doi:10.1111/j.1151-2916.1982.tb10782.x
32. Hagan JT (1979) J Mater Sci 14:2975. doi:10.1007/BF00611482
33. Lawn BR, Wilshaw R (1975) J Mater Sci 10:1049. doi:10.1007/BF00823224
34. Lawn BR, Swain MV (1975) J Mater Sci 10:113. doi:10.1007/BF00541038
35. Arora A, Marshall DB, Lawn BR, Swain MV (1979) J Non-Cryst Solids 31:415
36. Shannon RD (1976) Acta Cryst A 32:751. doi:10.1107/S0567739476001551
37. McMillan PW, Piriou B (1982) J Non-Cryst Solids 53:279
38. Chen Z-X, McMillan PW (1984) Phys Chem Glasses 25(5):142
39. McMillan PF, Sato RK, Poe BT (1998) J Non-Cryst Solids 224:267
40. Rocherullé J, Verdier P, Laurent Y (1989) Mater Sci Eng B2:265. doi:10.1016/0921-5107(89)90002-0
41. Loehman RE (1983) J Non-Cryst Solids 56:123
42. Schrimpf G, Frischat GH (1983) J Non-Cryst Solids 56:153
43. Cai Y, Thorpe MF (1989) Phys Rev B 40(15):10535. doi:10.1103/PhysRevB.40.10535
44. Thorpe MF (1983) J Non-Cryst Solids 57:355
45. Thorpe MF (1995) J Non-Cryst Solids 182:135
46. Avramov I, Keding R, Rüssel C (2000) Glastech Ber Glass Sci Technol 73(C1):138
47. Peter KW (1970) J Non-Cryst Solids 5:103